

Solving the Energy Management Problems Using Thermal Exchange Optimization

Zahia Djebblahi , Belkacem Mahdad , Kamel Srairi 

Department of Electrical Engineering, Laboratory of Energy Systems Modeling (LMSE), Science and Technology College, University of Biskra, Biskra, Algeria

Cite this article as: Z. Djebblahi, B. Mahdad and K. Srairi, "Solving the energy management problems using thermal exchange optimization," *Electrica*, 24(1), 67-86, 2024.

ABSTRACT

This paper proposes a new metaheuristic optimization algorithm, namely thermal exchange optimization (TEO), to solve the optimal power flow (OPF) problems. Various conflict objective functions, such as the total fuel cost (TFC), the total power loss, total emission gas (TEG), and the total voltage deviation have been optimized individually and simultaneously. The proposed TEO is validated on the electric test system Institute of Electrical and Electronics Engineers 30-Bus. The optimization results achieved by the proposed method in solving single-objective functions were more effective in finding the optimal solution compared to several well-known algorithms. The results clearly show the superiority of the proposed method in the majority of the case studies, with a better solution and competitive computational time. In contrast, the proposed multi-objective TEO (MOTEO) based OPF is investigated to solve the multi-objective OPF. It can be noticed from the results obtained that the proposed MOTEO achieved the better optimum compromise solution with a TFC value of 822.4796 \$/h and a TEG value of 0.26939 ton/h, which yields a competitive total cost (970.8219 \$/h) compared to those obtained by other algorithms. Moreover, the statistical analysis proves that the proposed MOTEO needs a lower number of trials to locate the best solution, also the standard deviation required to solve the single-objective problems is 0.03361, which is better compared to other techniques. The simulation results achieved by this method compared with other competitive algorithms proved the superiority of MOTEO in finding better solutions while also producing a high-quality Pareto front with appropriate precision.

Index Terms—Meta-heuristic algorithm, thermal exchange optimization (TEO), optimal power flow (OPF), IEEE 30-bus test system

I. INTRODUCTION

Nowadays, energy is an aspect of the development of every country, especially electrical energy, which has become necessary for most activities that would be almost impossible in its absence. As well as planning for the future growth of the power systems field, one of the most important challenges in power systems is the issue of optimal power flow (OPF) [1]. It is featured as an essential operator's tool, which plays a critical role in solving modern optimization problems related to the field of power system operation [2], and is useful for ensuring high efficiency and safety in real-time operations when increasing load demand is an urgent challenge for energy system operators. It aims to find optimum operating conditions subject to the physical, management, and engineering constraints of electrical grids [3], [4]. The OPF problem is generally considered to be a complex, non-linear, large-scale, multidimensional, non-convex optimization problem [5].

The main objective of the OPF strategy is to ensure the secure operation of the network. Especially while solving an OPF problem, it should govern the variables that control or make decisions in a practical area that optimizes predefined fitness functions [6]. The optimum value of the controlling variables, which is composed of the active powers generated, should be within a predetermined range [7]. Taking into consideration the satisfaction of a collection of equality and inequality constraints [8]. Typically, optimization focused on single-objective functions of OPF problems has been a means to address a function with a single goal. The total fuel generation cost is considered one of them, which is the most popular objective function and frequently calls for reducing generation costs in order to gain the maximum benefit of power dispatch. Furthermore, environmental and technological concerns have led to the consideration of various targets, including total emission gas (TEG). The active power loss should also be reduced as much as possible, and voltage deviation can reflect the quality of the voltage in the energy system; therefore, it should be reduced as much as possible [9]. With the aim of improving the security of energy systems and solving their problems more efficiently. The research is becoming

Corresponding author:

Zahia Djebblahi

E-mail:

zahia.djebblahi@univ-biskra.dz

Received: April 08, 2023

Revision Requested: May 1, 2023

Last Revision Received: October 5, 2023

Accepted: November 1, 2023

Publication Date: January 31, 2024

DOI: 10.5152/electrica.2024.23045



Content of this journal is licensed under a Creative Commons Attribution-NonCommercial 4.0 International License.

more and more motivating to study the multi objective optimal power flow (MOOPF), which aims to solve multiple objective functions simultaneously. Previously, traditional methods involved converting a single-objective problem into a multi-objective problem by assigning a weighting factor to each objective [10]. But recently, various multi-objective algorithms have been applied to solve real optimization problems.

The OPF has attracted many researchers to apply various optimization approaches that are dedicated to solving OPF problems. It can be classified into two different categories: the mathematical and metaheuristic approaches. Various mathematical methods have been used for optimizing various power flow problems, such as the interior point method, Newton's method, ϵ -constraint, nonlinear programming, quadratic programming, linear programming, and decomposition routines [11-14]. As the complexity of the problem increases, new techniques start via the Kuhn-Tucker condition to determine the optimal solution and converge in a few iterations to overcome the constraints. In general, the classical approaches have many weaknesses; for example, they suffer from certain obstructive limitations like the continuity and derivability of the fitness function and require much iteration, which leads to a long computational time to reach the near global solution. Also, those methods are based on mathematical concepts to deal with OPF problems of various sizes. Most of these methods can ensure a local optimum but lack the ability to achieve a global solution [15].

In order to reduce and overcome the drawbacks of those approaches, the researchers have developed various techniques that have employed unpopular research domains, especially to solve complex power-engineering optimization problems, which include the OPF problems [16]. In the past few years, numerous meta-heuristic algorithms have been widely employed for solving several optimization problems. Nature is considered to be a major source of inspiration for numerous algorithms. These algorithms are unique and can be applied to each optimization problem regardless of its origin; they are aimed at simplifying and rapidly solving complex problems [17]. They are different from the traditional techniques, which can provide a unique solution; those methods have been implemented based on various natural phenomena like biological, physical, and chemical phenomena [18].

Several optimization algorithms have been applied to solving the OPF problem and have taken up a large place in the literature. Generally, metaheuristic algorithms are commonly developed and successfully applied for solving the classical OPF problem [19], ranging from traditional methods. Some of them have been classified as evolutionary algorithms, biological phenomena, swarm algorithms, and others based on physical phenomena, etc., like the genetic algorithm (GA) [20], particle swarm optimization (PSO) [21], bacterial foraging methods, such as bat algorithms (Bat) [22]. In [23], a recent algorithm named enhanced equilibrium optimizer is proposed to solve several optimal power flow (OPF) problems. It was clearly proven its efficacy compared to other powerful optimization methods. The effectiveness of this method is analyzed and assessed on the standard IEEE 30-bus system, obtained results compared to many optimization algorithms [24], enhanced GAs [1], etc. Although various hybrid metaheuristic algorithms have been developed and continue to be developed every day, some of them are used in solving different optimization problems, and most are not applied in the new studies. These methods are not widely used, and do not achieve

the expected effect, which is assigned of a serious failure, not only for these hybrid metaheuristic algorithms but also for any newly developed algorithms for the first time [25]. Hybrid algorithms have been applied for solving the OPF problem like, particle swarm with gray wolf optimizer [14], the hybrid PSO and Gravitational search algorithm (GSA) [26], and hybrid Differential Evolution (DE) with harmony search algorithm (HSA) [27]. In [28], a physics-guided graph convolutional neural network (GCNN) algorithm was employed to solve the OPF, taking into account various changes in topologies. An iterative feature of physical and practical constraints is also developed. The efficiency of the proposed technique validated on several IEEE test systems such as the IEEE 57-bus system, the IEEE 118-bus, and the 300-bus. In [29], a hybrid Harrison Hawk optimization based on differential evolution algorithm has been developed to solve engineering problems. This algorithm is particularly effective in solving the OPF problem on the IEEE 30-bus system; this algorithm is more effective in finding the optimal solution. In [30], a new hybrid algorithm based on combining the teaching learning-based artificial bee colony (TLABC) with the fitness-distance balance-based-TLABC (FDB-TLABC) is proposed to solve single-objective OPF, by considering the integration of renewable sources and FACTS devices. The obtained results using FDB-TLABC proves its competitive aspect in solving with accuracy the optimal power flow problem. This algorithm has a distinct advantage over its competitors in terms of finding optimal solutions. In [31], a hybrid method namely fitness-distance balance-based artificial ecosystem optimization (FDB-AEO) designed and applied to improve the solution of the transient stability constrained OPF problem. In [32], a recent hybrid technique named fitness-distance balance-based adaptive guided differential evolution algorithm was developed and applied for solving the security-constrained OPF; the performance of this method was validated on an IEEE 30-bus test system under several operational conditions. Furthermore, some multi-objective algorithms have been suggested for solving the OPF problem, comprising two or more fitness functions like the non-dominated sorting GA [33], multi-objective PSO (MOPSO) [34] and the multi-objective grasshopper optimization algorithm [8]. In [35], a powerful and stable method called multi-objective adaptive guided differential evolution (MOAGDE) was used for solving the MOOPF and can find the best Pareto optimum solutions. In [36], a recent multi-objective version named improved multi-objective manta-ray foraging optimization (IMOMRFO), has the ability to achieve the best compromise solution with high efficiency and precision. These modern optimization techniques can mostly be used to solve the OPF problem and have proven their high performance in several power-engineering optimization problems.

This research paper contributes to the study of the effectiveness of a newly emerged metaheuristic algorithm called thermal exchange optimization (TEO) for solving OPF problems with both single- and multi-objective types. The performances of the proposed method have been validated on many practical optimization problems. This algorithm is examined in IEEE 30-bus system, and the results of optimization demonstrate the superiority of the present technique with success in solving the OPF problem in order to find a better solution with less iteration and a minimum execution time. The obtained results using the proposed TEO have been compared to particular metaheuristic techniques, such as the GA, which mimics genetic laws to provide the best solutions [37], and the PSO, this algorithm was developed based on the behavior of animals. Where, the candidates (solutions) tend to track the best individual

experience as well as the global best solution experimented by all candidates up until each iteration, which was developed based on the behavior of animals, and to the salp swarm algorithm (SSA) which is a recent intelligence algorithm-based swarm [38]. On the other hand, the proposed algorithm namely TEO has been compared to other recent hybrid algorithms such as, the FDB-AEO [32], and FDB-based Archimedes optimization algorithm (FDB-AOA), the purpose of using this technique is to investigate how the FDB-based guide selection technique affects the exploitation and exploration stages of the AOA algorithm, also to identify the guidance mechanism that delivers the most efficient search results [39]. The obtained results clearly show that the proposed TEO can be used to solve with accuracy various single-objective functions related to the OPF problems.

A second goal of this article is the implementation of the recent version of multi-objective TEO to handle MOOPF problems. To verify their performances relentlessly, a comparative study between the reported method and other multi-objective versions of some algorithms, like the multi-objective GA (MOGA), which used a non-dominated sorting process to assign labels to Pareto sets, beginning with the initial solution, is illustrated using the Pareto fronts. In contrast, the set of optimum Pareto is a collection of non-dominated solutions frontier. The corresponding objective function's values in the objective space are called the Pareto front [40]. Another popular algorithm with high performance is MOPSO. This algorithm generates a repository with a defined capacity in which a set of non-dominated solutions accumulated for use in the next steps [41]. The multi-objective SSA (MSSA) starts with a foraging strategy by preparing a random initial population of salps, respecting the limits and boundaries of variables. Afterward, it computes the fitness function value for each salp to provide non-dominated solutions in the repository. A roulette wheel is used to archive non-dominated solutions. Following that, the positions of the leading/following salps are then updated to ensure the best compromise in terms of multiple objectives before the end condition is satisfied [42]. The MOAGDE is a robust and efficient method for discovering Pareto-optimal solutions for multi-objective optimization problems, involving various forms with complex decision and objective spaces. It emerged by adapting the adaptive guided differential evolution algorithm specifically for multi-objective optimization. Although this method was rarely studied, the OPF remains a significant challenge in the planning and operation of contemporary power systems. The efficacy of this method (MOAGDE) was examined on various fitness functions on an IEEE 30-bus test system; the details of this method can be seen in [35]. The IMOMRFO is a highly efficacious technique that was created using the Pareto archiving approach, which is based on crowding distance [36]; the proposed approach was used for handling a multi-objective optimization problem in the engineering field and also for solving the MOOPF. The effectiveness of this developed method was examined on an IEEE 30-bus system. The details of this method can be seen in [43]. The obtained results using the proposed multi-objective TEO (MOTEO) compared to other recent algorithms clearly proves its high ability to find with accuracy the best Pareto front solution of various conflict objective functions.

The rest of this research paper is detailed as follows:

A brief description of the OPF formulation is presented in the first section. The second section presents the proposed thermal exchange algorithm and their recently investigated multi-objective version

(MOTEO) for solving the OPF problems with both single- and multi-objective types. The simulation and numerical results based on the practical test system IEEE 30-bus are presented and discussed in the third section; the improvement results are clarified and discussed in the fourth section. Finally, the last section provides the conclusions and future directions.

II. DESCRIPTION OF THE OPTIMAL POWER FLOW PROBLEM

The OPF is a leading energy management optimization tool that aims to minimize a nonlinear fitness function and finds the optimal configuration of numerous control variables while keeping all equality and inequality constraints within their specified maximum and minimum boundaries [11], [44]. In general, the OPF problem can be formulated as follows:

$$\text{Optimize } F(x, u) \text{ (is the fitness function)} \quad (1)$$

subjected to

$$G(x, u) = 0 \text{ (is the equality_constraints)} \quad (2)$$

$$H(x, u) \leq 0 \text{ (is the inequality_constraints)} \quad (3)$$

Here, F denotes the modeled fitness function; u indicates the decision variables; and x indicates the state variables [7]. The vector of state variables is expressed using the following equation [3-4]:

$$x = [P_{G1}, V_{L1}, \dots, V_{L,NPQ}, Q_{G1}, \dots, Q_{G,Ng}, S_{TL1}, \dots, S_{TL,NL}] \quad (4)$$

where P_{G1} indicates the slack bus's power, V_L denotes the load bus's voltage, Q_G represents the generator's reactive power, and S_{TL} indicates the apparent power flow in transmission lines. NPQ indicates the total number of load bus, a generation bus number is indicated by N_{G1} and a transmission line by NTL. The controlled variables (u) can be formulated as follows [3, 4]:

$$u = [P_{G2}, \dots, P_{G,Ng}, V_{G1}, \dots, V_{G,Ng}, Q_{C1}, \dots, Q_{C,nc}, T_1, \dots, T_{N_{Tr}}] \quad (5)$$

where P_G denotes the vector of output real power of thermal generating units, V_G refers to the generator's bus voltage, Q_C indicates the injected shunt compensator's reactive power, T denotes the transformer's tap setting, n_c represents the shunt reactive compensation unit number, and N_{Tr} is the transformer number.

A. Fitness Functions

In this research paper, there are four fitness functions related to power system operation: the total fuel cost (TFC), TEG, total active power losses (APL), and total voltage deviation (TVD) [10-12]. Their mathematical models can be expressed as follows:

1) Minimization of Total Fuel Cost

The first fitness function is to minimize the TFC ($Min.f_{TFC}$) of generators units (\$/h), and the fitness function-based quadratic form is expressed as follows [5-6], [15]:

$$f_1 = Min.f_{TFC}(x, u) = \sum_{i=1}^{N_G} a_i P_{G_i}^2 + b_i P_{G_i} + c_i \quad (6)$$

where N_G refers to the number of generators and P_{G_i} indicates the active power output of i th generating units.

a_i , b_i , and c_i denote the coefficients of cost function-based thermal generating units.

2) Minimization of the Total Emission Gas

The second fitness function is to reduce the emission of gas ($Min.f_{TEG}$). It can be stated as follows (eq. 7) [5] [16]:

$$f_2 = Min.f_{TEG}(x,u) = \sum_{i=1}^{N_G} 10^{-2} (\alpha_i + \beta_i P_{G_i} + \gamma_i P_{G_i}^2) + \zeta_i \exp(\lambda_i P_{G_i}) \quad (7)$$

where: α_i , β_i , γ_i , ζ_i , and λ_i denote the coefficients of fitness function emission gas of i th generating units.

3) Minimization of Total Active Power Loss

The third fitness function is the total APL which can be formulated using the following equation [4]:

$$f_3 = Min.f_{APL}(x,u) = Min \left[\sum_{i=1}^{NTL} G_{ij} (V_i^2 + V_j^2 - 2V_i V_j \cos \theta_{ij}) \right] \quad (8)$$

where V_i indicates the magnitude of voltage at i th bus, G_{ij} denotes the conductance between bus i and bus j , NTL is the transmission lines number, and θ_{ij} is the voltage angle difference [4].

4) Minimization of Voltage Deviation

The last fitness function is voltage deviation. With a goal for limiting the magnitude of voltage deviation at the load buses nearly to the 1.0 p.u., it can be expressed as follows [6], [10], [15], [45], [46]:

$$f_4 = VD = \sum_{i=1}^{NPQ} |V_i - 1| \quad (9)$$

where VD represents the voltage deviation, NPQ is the load buses numbers, and V_i denotes the voltage in each load bus.

B. Multi-Objective Functions

The multi-objective problems can be defined as problems in which there are several independent fitness functions that are optimized simultaneously. This can be expressed by the following equation [44]:

$$MinF(x,u) = [F_1(x,u), F_2(x,u), \dots, F_i(x,u)] \quad (10)$$

where i is the number of objective functions.

C. System Constraints

To achieve the above objectives optimally, a collection of equality and inequality restrictions must be satisfied.

1) Equality Constraints

The equality constraints reflect the physical proprieties of the power system. These constraints can be enforced through the power flow equations, which require that the net injection of active and reactive power at each bus is equal to zero [1]. A power system's operating limits are determined by its equipment. It is possible to categorize equality constraints as follows [6], [47]:

$$P_{G_i} - P_{D_i} = V_i \sum_{j=1}^{N_b} V_j (G_{ij} \cos(\theta_{ij}) + B_{ij} \sin(\theta_{ij})) \quad (11)$$

$$Q_{G_i} - Q_{D_i} = V_i \sum_{j=1}^{N_b} V_j (G_{ij} \sin(\theta_{ij}) - B_{ij} \cos(\theta_{ij})) \quad (12)$$

where; P_{D_i} , Q_{D_i} denote the active and reactive power demand of the i th bus; respectively; G_{ij} , B_{ij} represent the conductance and susceptance of transmission line between i and j buses; respectively; θ_{ij} denotes the voltage phase angle difference between buses i and j ; V_i and V_j denote the magnitudes of voltage at i th and j th bus; N_b represents the total number of buses.

2) Inequality Constraints

1. Generation constraints: active power (eq. 10), reactive power (eq. 11), and voltage (eq. 13) [6], [47]

The output power of each generating unit has a lower and upper bound, and this constraint is expressed by using, [40], [46]:

$$P_{G_i}^{min} \leq P_{G_i} \leq P_{G_i}^{max} \quad (13)$$

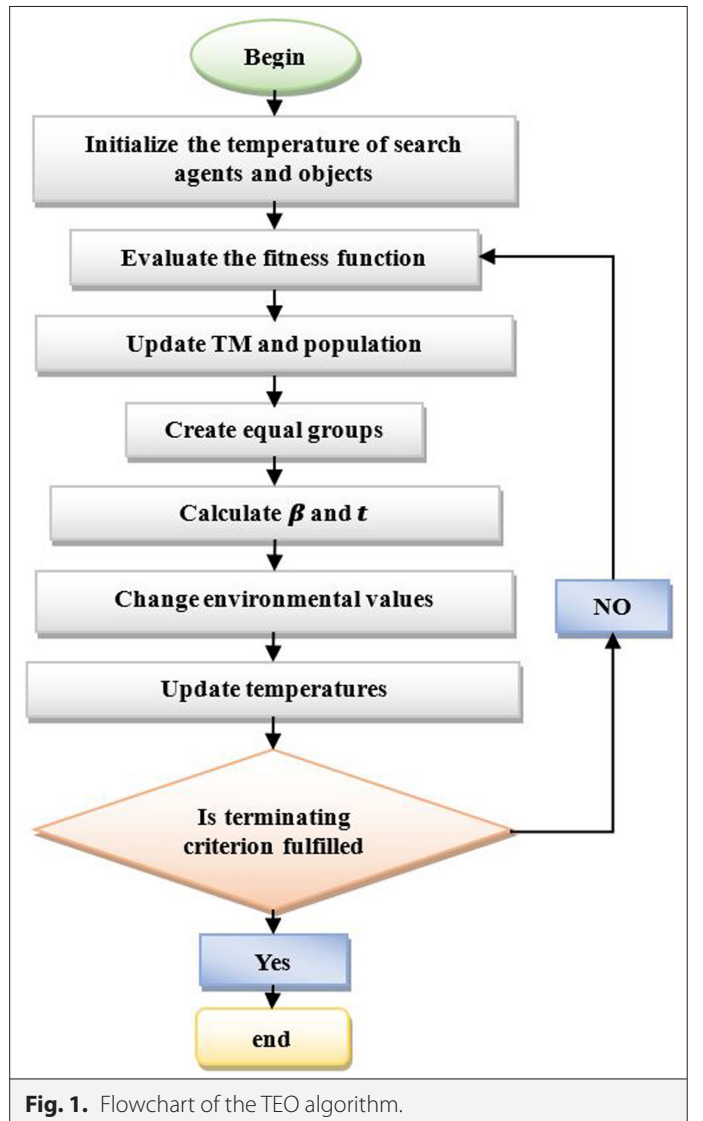


Fig. 1. Flowchart of the TEO algorithm.

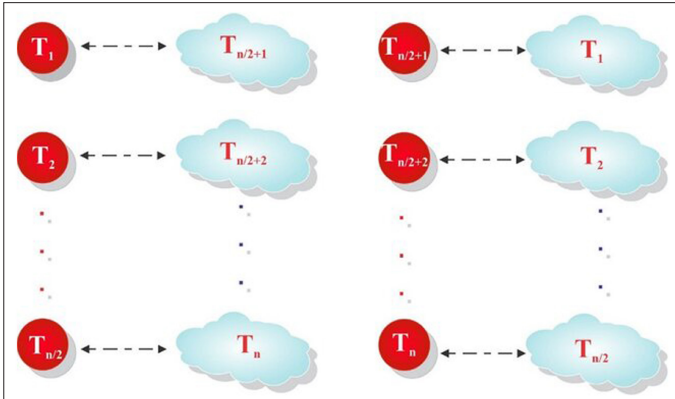


Fig. 2. Pairing cooling objects and environmental solutions.

$$Q_{G_i}^{min} \leq Q_{G_i} \leq Q_{G_i}^{max} \quad (14)$$

$$V_{G_i}^{min} \leq V_{G_i} \leq V_{G_i}^{max}; \quad i = 1, 2, \dots, N_G \quad (15)$$

1. Security constraints

These constraints include the limits on voltage magnitudes of load bus (V_{L_i}), power transmission line limit (S_{L_i}), and tap setting transformer ($T_{Tr,j}$) constraints [38].

$$|S_{L_i}| \leq S_{L_i}^{max}; \quad i = 1, 2, \dots, N_{STL} \quad (16)$$

where S_{L_i} and $S_{L_i}^{max}$ are the power boundaries of the i th transmission line. N_{STL} is the number of transmission lines of the power system [6], [29].

- Load bus: voltage magnitudes of load buses [4], [6], [10], [44], [47]

$$V_{L_i}^{min} \leq V_{L_i} \leq V_{L_i}^{max}; \quad i = 1, 2, \dots, NPQ \quad (17)$$

Where $V_{L_i}^{min}$ and $V_{L_i}^{max}$ are the boundaries voltage limits of the i th load bus V_{L_i} . NPQ is the number of load buses.

- Transformer tap setting: [6], [47]

$$T_{Tr,j}^{min} \leq T_{Tr,j} \leq T_{Tr,j}^{max}; \quad i = 1, 2, \dots, N_{Tr} \quad (18)$$

where $T_{Tr,j}^{min}$ and $T_{Tr,j}^{max}$ indicate the boundaries of the i th tap changer transformer. N_{Tr} is the number of tap changers.

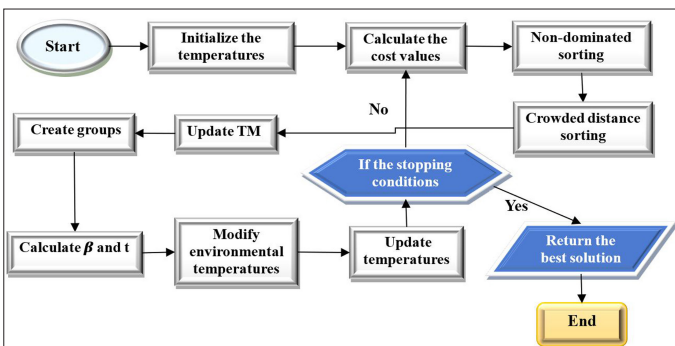


Fig. 3. Flowchart of the proposed MOTEO algorithm.

TABLE I TEST CASES ADDRESSED IN THIS RESEARCH

Test case n°	Fitness Functions
Test case 1	Total fuel cost (TFC)
Test case 2	Total emission gas (TEG)
Test case 3	Active power losses (APL)
Test case 4	Voltage deviation (VD)
Test case 5	TFC and TEG simultaneously
Test case 6	TFC and APL simultaneously
Test case 7	APL and VD simultaneously
Test case 8	TFC, TEG, and APL simultaneously

1. Shunt capacitor: reactive power of the shunt capacitor must (eq. 19) [6], [10]

$$Q_{C_j}^{min} \leq Q_{C_j} \leq Q_{C_j}^{max}; \quad i = 1, 2, \dots, n_C \quad (19)$$

where $Q_{C_j}^{min}$ and $Q_{C_j}^{max}$ are the boundaries of the i th shunt compensator Q_{C_j} . n_C is the number of shunt capacitors connected to the power system.

III. THE PROPOSED METAHEURISTIC OPTIMIZATION ALGORITHM

The main purpose of this study is to adapt and apply a new efficient physics-inspired meta-heuristic optimization algorithm, namely TEO, introduced recently by *Kaveh* and *Dadras* in 2017 [48], to solve vari-ous single- and multi-objective OPF problems.

A. Thermal Exchange Optimization

The TEO is inspired by physical phenomena to solve an optimization problem [48]. The proposed TEO is based on the concept of the Newton's law of cooling to find the best optimum solution. The process of this method is based on the behaviors of objects according to their temperature, which affects their position, switching between warm and cold to reveal an updated position [49]. In the TEO optimizer, the search agents are divided into two parts. The first

TABLE II DETAILED DATA OF THE IEEE 30-BUS TEST SYSTEM

Element	Quantity	Details
Buses-number	30	-
Branches-number	41	-
Generators-number	6	Slack-Bus is 1/ 2/ 5/ 8/ 11 and 13
Capacitors-number	9	buses: 10 and 24
Transformer with tap changer	4	branches: 11/ 12/ 15 and 36
Total power demand		
Active power	-	283.4 MW
Reactive power	-	126.2 MVAR
Load buses	24	-

TABLE III THE COST COEFFICIENTS OF GENERATING UNITS OF IEEE 30-BUS SYSTEM

Bus	c_i	b_i	a_i	$P_{G_i}^{min}$	$P_{G_i}^{max}$
1	0.00375	2	0	50	200
2	0.0175	1.75	0	20	80
5	0.0625	1	0	15	50
8	0.00834	3.25	0	10	35
11	0.025	3	0	10	30
13	0.025	3	0	12	40

part presents the candidate search agents, which are considered as cooling objects whose temperature represents the optimizing variables; the other part is considered the remaining agents supposed to represent the environment [48], [49] and then the reverse process [48]. The following steps are used to explain the original TEO algorithm. The flowchart of the reported method TEO is depicted in the Fig. 1:

The process of this algorithm starts with the initialization of the temperatures of all search agents and objects, which are randomly created in the search space [2]. Their solutions can be described as in equation (20) [48].

$$T_k^0 = T_{Min} + rand_k \cdot (T_{Max} - T_{Min}) \quad k = 1, \dots, N \quad (20)$$

where $T_k^0 = T_{Min} + rand_k \cdot (T_{Max} - T_{Min})$ $k = 1, \dots, N$ represents the initial vector solution of the k th object; T_{Max} and T_{Min} are the boundaries of the solution vector; $rand_k$ is a vector of random numbers created independently for the k th object, where each component ranges between 0 and 1, and N is the number of objects or search agents [48];

After then, the temperatures of all objects are evaluated and descendingly organized according to their value of the cost function, while preserving the first N_{pop} number of objects to be equal to the number of presumed objects. The historically best solutions must be saved in thermal memory (TM) in order to achieve a higher efficacy and lower complexity; They are updated and renewed with each iteration [48].

TABLEE IV THE EMISSION COEFFICIENTS OF GENERATING UNITS OF IEEE 30-BUS TEST SYSTEM

Bus	$\gamma \cdot 10^{-2}$	$\beta \cdot 10^{-4}$	$\alpha \cdot 10^{-6}$	$\nu \cdot 10^{-4}$	$\lambda \cdot 10^{-2}$
1	4.091	-5.554	6.49	2.0	2.857
2	2.543	-6.047	5.638	5.0	3.333
5	4.258	-5.094	4.586	0.01	8.0
8	5.326	-3.55	3.38	20.0	2.0
11	4.258	-5.094	4.586	0.01	8.0
13	6.131	-5.555	5.151	10.00	6.667

The sorted objects are divided into two equal parts according to the definition in Fig. 2. At this time, the first half T_1 is an environment object $T_{\frac{n}{2}+1}$, and the second half is the cooling object.

According to Newton's law of cooling, the rate of heat loss of an agglomerated object is exactly proportional to the temperature difference between the object and its surroundings, as expressed in the equation below (Eq. 21).

$$\frac{Te(t) - Te_{Env}}{Te_0 - Te_{Env}} = \exp(-\beta t) \quad (21)$$

where $Te(t)$ represents the novel temperature at time t following the thermal exchange between an object with the temperature Te_0 and the environment with temperature Te_{Env} . β is a constant that relates to several parameters, such as heat capacity and object-specific density. As can be observed, when β has a higher value, the object tends to change less amount of temperature. An analogy is inspired by this feature.

β is defined to minimize the solution's cost and variance. The value β is expressed as in the following equation (eq. 22):

$$\beta = \frac{f_i}{f_{max}} \quad (22)$$

where f_i represents the cost of the current object and f_i is the highest cost of the worst object in the population, respectively. t is the time associated with the iteration numbers, as illustrated in the following equation (eq. 23).

$$t = \frac{\text{Iter}}{\text{Max-Iter}} \quad (23)$$

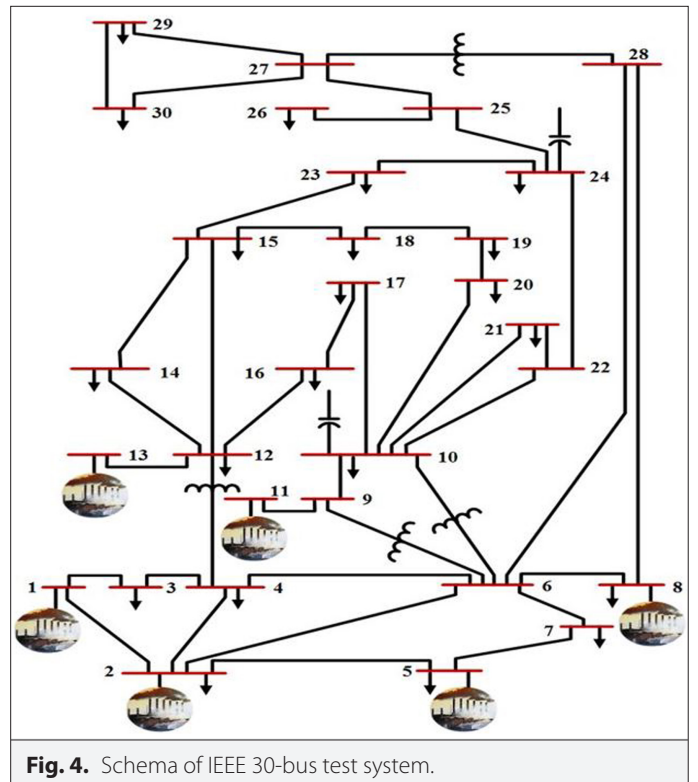


Fig. 4. Schema of IEEE 30-bus test system.

TABLE V INTERNAL PARAMETER SETTINGS OF THE ALGORITHMS

	Algorithm Name	Parameters	Value
Single objective	All algorithms	Population size	20
		Maximum iterations	200
	GA	Selection type	Roulette
		Crossover	0.8
		Mutation	0.14
	PSO	Inertia weight (w1)	0.5
		Inertia weight (w2)	0.9
		Local weight (C1)	1.2
		Local weight (C2)	1.4
	SSA	C1	[0, 1]
		C2	Rand ()
		C3	Rand ()
	TEO	C1	1.2
		C2	2.2
FDB-AEO	The standard parameters of the algorithm		
FDB-AOA	The standard parameters of the algorithm		
Multi-objective	MOGA	The same parameters of single-objective	
	MOPSO	c1	1.2
		c2	1.4
		Beta	0.1
		Lambda	0.9
		w	1
		wdamp	0.95
	MSSA	The same parameters of single-objective	
	MOTEO	C1	1.2
		C2	2.2
		Percentage of crossover	0.7
Percentage of mutation		0.4	
MOTEO	Mutation		0.02
	DSC-MOAGDE	The standard parameters of the algorithm	
IMOMRFO	The standard parameters of the algorithm		

GA, genetic algorithm; FDB-AEO, fitness-distance balance-based artificial ecosystem optimization; FDB-AOA, fitness-distance balance- based Archimedes optimization algorithm; IMOMRFO, improved multi-objective manta-ray foraging optimization; MOGA, multi-objective genetic algorithm; MOPSO, multi-objective particle swarm optimization; MSSA, multi-objective salp swarm algorithm; MOTEO, multi-objective thermal exchange optimization; PSO, particle swarm optimization; SSA, salp swarm algorithm; TEO, thermal exchange optimization; DSC-MOAGDE: Dynamic Switched Crowding mutiobjective-Adapative Guided Differential Evolution Algorithm.

where $Iter$ is the current iteration, and $Max - Iter$ is the maximum number of iterations.

The environmental solutions have been randomized change before updating the temperature using the eq. (24) [48].

$$T_i^{Env} = (1 - (C_1 + C_2 \times (1 - t)) \times Rand) \times T_i^{Env} \quad (24)$$

where T_i^{Env} and T_i^{Env} indicate the object's temperature before and after modification; C_1 and C_2 are the internal control parameters; $rand$ is a random vector comprising in the interval [0 1]. Equation 25 is used for checking the new temperature of each agent, which is a essential step was designed to minimize randomness when the algorithm approaches their final iterations, hence, decreasing and increasing exploitation [49].

$$T_i^{New} = T_i^{Env} + (T_i^{Env} - T_i^{Old}) \times \exp(-\beta \times t) \quad (25)$$

where T_i^{Old} and T_i^{New} denote the previous and updated temperature of the i th object, and β and t are the two parameters mentioned above.

The second mechanism for escaping local optima was created to find a global optimum solution. This mechanism is introduced through the parameter 'Pro,' which takes values within the range (0, 1), specifying whether one component of each cooling object needs to be replaced or not. Each agent Pro value is compared to $Ran(i)$, where i ranges from (1 to n) is a random number uniformly distributed between (0 and 1). If $Ran(i) < Pro$, one dimension of the i th agent is randomly selected and its value regenerated as follows using Equation 26 [48]:

$$T_i^j = T_j^{min} + random \cdot (T_j^{max} - T_j^{min}) \quad (26)$$

TABLE VI THE OPTIMIZED RESULTS OF THE TEO ON SOLVING SINGLE-OBJECTIVE OPF PROBLEM

	Test Case 1	Test Case 2	Test Case 3	Test Case 4
PG1	176.4878	70.1690	51.9111	173.1889
PG2	48.8374	71.4234	79.9957	71.4215
PG5	21.4310	49.1068	49.9983	15.0800
PG8	21.9482	34.6021	34.9973	11.4022
PG11	12.1969	28.2083	29.9984	10.7081
PG13	12.0000	33.8037	39.9968	12.0000
Total fuel cost(\$/h)	802.3607	929.7806	968.5297	815.1328
Emission gas (ton/h)	0.3665	0.21929	0.2216	0.3673
Active power losses (MW)	9.5012	3.9134	3.4976	10.4008
ΔV (p.u.)	0.6829	0.7219	0.7237	0.67514
CPU time (s)	16.9921	17.28617	17.2302	17.0174

Bold values in Table X indicate the best value obtained.

TABLE VII THE OPIMIZED RESULTS OF THE PRESENTED METHOD (TEO) WITH OTHER METHODS: TEST CASE 1

	GA	PSO	SSA	FDB-AEO	FDB-AOA	TEO
PG1	172.7648	178.2879	176.8127	176.6824	176.9304	176.4878
PG2	52.0187	48.5015	48.7627	48.8565	49.5669	48.8374
PG5	22.9486	21.4564	21.5116	21.5157	21.3281	21.4310
PG8	20.9285	20.2835	21.7192	21.6382	20.5942	21.9482
PG11	10.8531	11.9820	12.1158	12.2217	12.5504	12.1969
PG13	13.2136	12.5260	12.0000	12.0013	12.0000	12.0000
Total fuel cost (\$/h)	802.8716	802.4219	802.3603	802.3604	802.3883	802.3607
Emission gas (ton/h)	0.3544	0.3715	0.3674	0.3671	0.3678	0.3665
Active power losses (MW)	9.3273	9.6373	9.5220	9.5157	9.5700	9.5012
ΔV (p.u.)	0.6817	0.6823	0.6827	0.6828	0.6829	0.6829
CPU time (s)	22.7751	18.2526	17.5517	17.3033	18.5131	16.9921

GA, genetic algorithm; FDB-AEO, fitness-distance balance-based artificial ecosystem optimization; FDB-AOA, fitness-distance balance-based Archimedes optimization algorithm; PSO, particle swarm optimization; SSA, salp swarm algorithm; TEO, thermal exchange optimization. Bold values in Table X indicate the best value obtained.

Stopping criteria of the algorithm

It must be controlling the maximum number of iterations; if the condition is met, the algorithm stops searching and reports the best solution found so far; otherwise, it resumes and returns the stage of evaluation of temperature. The optimization process is completed after several iterations [49].

B. Multi-objective thermal exchange optimization

Due to structural similarity to a single-objective TEO, just the necessary difference is mentioned for the sake of brevity. The differences between the introduced MOTEO and its basic single-objective version are mainly relied upon in how the objects are arranged and how the parameter β is measured. β is restructured as follows (eq. 27) [49]:

$$\beta = \frac{r_i}{N_{Pop}} \quad (27)$$

where r_i reports the final rank of the solution and N_{Pop} refers to the number of population.

n TEO, the highest i parameter is related with the increasing cost value of the solution (see Eq. 19). In MOTEO, each solution requires a number of cost values, whereas in TEO, each solution has a multiple cost value. As a result, the novel formulation (Eq. 25) is suggested, which functions similarly. The solution that belongs to a larger rank of Pareto front has a higher β parameter.

The reminder steps are similar to TEO. The flowchart in Fig. 3 explains the basics of MOTEO. The details of MOTEO can be retrieved from [48].

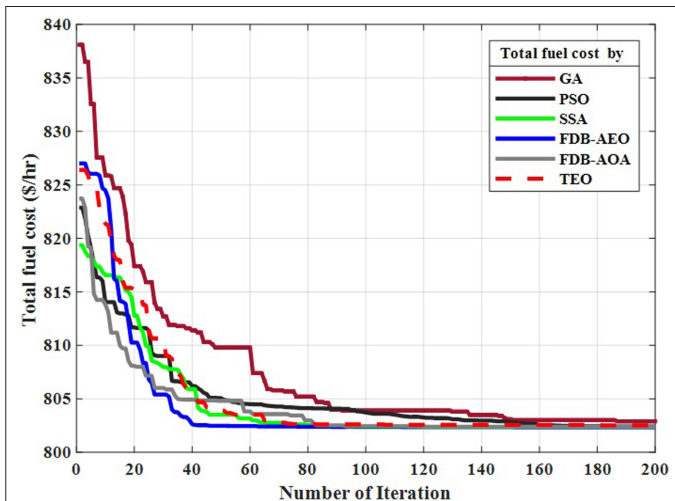


Fig. 5. Convergence characteristics for TFC minimization: test case 1.

IV. SIMULATION PROCEDURE

The performances of the proposed TEO have been validated on the standard IEEE 30-bus test system. Eight different test cases have been addressed, which are mentioned in Table I. The simulations have been elaborated using PC-HP-Intel (R) Core (TM) i5-1035G1 CPU@1.00 GHz to 1.19 GHz, with a RAM of 8 GB under Windows 10, 64-bit, and MATLAB 2021.

A. Brief Description of IEEE 30-Bus Test System

The detailed data of this test system are mentioned in Table II. Also, the other data of the test system, including the cost and emission generator coefficients and output generation power boundary limits, are indicated in Tables III and IV. Fig. 4 illustrates the topology of the IEEE 30-bus test system [13], [29].

B. Numerical Simulation Results and Discussion

To achieve a rational comparison, all test-cases and all the algorithms used are compared under the same conditions, such as the

TABLE VIII THE OPTIMIZED RESULTS OF THE PRESENTED METHOD (TEO) WITH OTHER METHODS: TEST CASE 1

PGi (MW)	GA	PSO	SSA	FDB-AEO	FDB-AOA	TEO
PG1	70.1690	68.8179	68.1098	68.2291	68.3633	70.5539
PG2	71.4234	70.9642	71.2237	71.3491	72.2541	68.2759
PG5	49.1068	50.0000	50.0000	49.9992	49.9968	50.0000
PG8	34.6021	35.0000	35.0000	34.9990	34.9782	35.0000
PG11	28.2083	30.0000	30.0000	29.9988	29.9980	30.0000
PG13	33.8037	32.4405	32.8757	32.6383	31.6380	33.4010
Total fuel cost (\$/h)	929.7806	934.0096	935.3462	935.0626	934.5488	931.5967
Emission gas (ton/h)	0.21929	0.21756	0.21756	0.2176	0.2176	0.2137
Active power losses (MW)	3.9134	3.8225	3.8092	3.8136	3.8285	3.8308
ΔV (p.u.)	0.7219	0.7236	0.7237	0.7237	0.7235	0.7238
CPU time (s)	20.55941	18.47389	17.2877	18.1378	17.9821	17.2861

GA, genetic algorithm; FDB-AEO, fitness-distance balance-based artificial ecosystem optimization; FDB-AOA, fitness-distance balance-based Archimedes optimization algorithm; PSO, particle swarm optimization; SSA, salp swarm algorithm; TEO, thermal exchange optimization. Bold values in Table X indicate the best value obtained.

maximum iteration being 200 iterations and the population size being 20. The rest of the parameter settings of the algorithms used in this work have been mentioned in Table V.

For all test cases, the simulation results include the optimal settings of the control variables, the TFC, TEG, APL, and voltage deviation.

• Solution Methodology

The basic steps for solving OPF using metaheuristic optimization methods are:

Step 1: Define the fitness function and the constraints.

Step 2: Introduce the matrix data lines and line data of the test system.

Step 3: Initialization of the parameters of the metaheuristic, such as the population size and boundary limits of the decision variables. This population consists of a set of solution vectors, each representing a possible configuration of the power system variables (e.g., generator setpoints, transformer tap positions).

Step 4: Evaluation of the fitness of each candidate solution in the population. Fitness is determined by calculating the objective function value for each solution and checking if it satisfies the constraints. Solutions that violate constraints can be assigned a penalty or a low fitness value.

Step 5: Evaluate the fitness fiction by calculating the power flow in order to find the best global optimal solution.

Step 6: Apply the exploration stage and the exploitation stage

Step 7: Update the solution and save the best decision variables.

Step 8: Test convergence criteria.

1) Single-Objective Optimal Power Flow Problem

The efficacy of the proposed TEO was first evaluated by testing it on solving single-objective OPF problems, which were considered as test cases 1 to 4 and discussed previously in Table I. Table VI represents the details of the simulation results for each test case.

To demonstrate the superiority of this algorithm (TEO), their simulation results compared with the other algorithms have proven their effectiveness for solving the OPF problems, such as the SSA, PSO, and GA.

• Test Case 1: Minimization of the TFC

The first test case selected the TFC as a fitness function. Table VII displays the simulation results of the presented technique compared

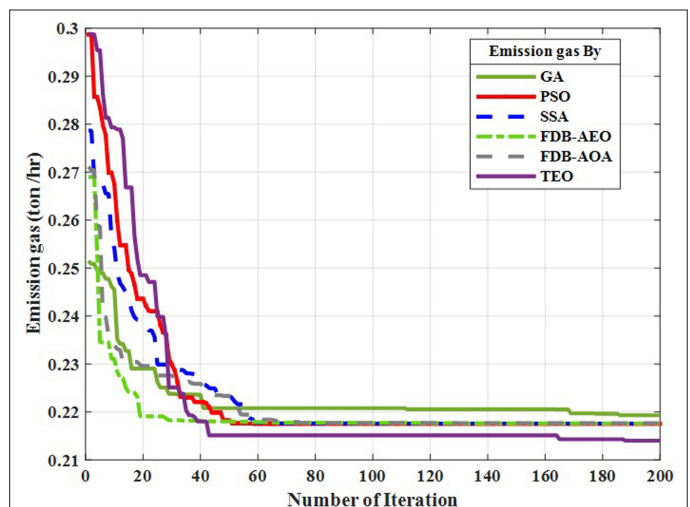


Fig. 6. Convergence behaviors for TEG minimization: test case 2.

TABLE IX THE OPTIMIZED RESULTS OF THE PRESENTED METHOD (TEO) WITH OTHER METHODS: TEST CASE 3

PGi (MW)	GA	PSO	SSA	FDB-AEO	FDB-AOA	TEO
PG1	55.74086	53.2708	51.9292	52.4025	52.3605	51.9111
PG2	78.40561	79.4866	79.9865	79.7951	79.7951	79.9957
PG5	49.90884	49.6869	49.9955	49.9487	49.9887	49.9983
PG8	34.30025	34.9979	34.9982	34.9731	34.9931	34.9973
PG11	28.80385	29.8611	29.9940	29.9224	29.9124	29.9984
PG13	39.81672	39.6225	39.9946	39.8647	39.8547	39.9968
Total fuel cost (\$/h)	960.9912	964.7394	968.4830	967.3385	967.5097	968.5297
Emission gas (ton/h)	0.2216	0.2213	0.2216	0.3663	0.3662	0.216
Active power losses (MW)	3.5761	3.5259	3.4979	3.5065	3.5045	3.4976
ΔV (p.u.)	0.7225	0.7236	0.7237	0.7236	0.7236	0.7237
CPU time (s)	21.7652	18.7029	17.3293	17.3758	17.5368	17.2302

CPU, Central Processor Unit; GA, genetic algorithm; FDB-AEO, fitness-distance balance-based artificial ecosystem optimization; FDB-AOA, fitness-distance balance-based Archimedes optimization algorithm; PSO, particle swarm optimization; SSA, salp swarm algorithm; TEO, thermal exchange optimization. Bold values in Table 9 indicate the best value obtained.

with other techniques. The values of the best TFC are almost the same by all method, especially by SSA, FDB-AEO, FDB-AOA, and TEO. It is confirmed that the TEO achieved the best TFC (802.3606831 \$/h) at a reduced execution time compared to other techniques. The convergence behaviors for TFC minimization using the TEO, and using other methods are illustrated in Fig. 5.

• **Test Case 2: Minimization of Total Emission Gas**

For the second test case, the fitness function selected is the TEG. The optimized results provided by the presented technique (TEO) compared with others are depicted in Table VIII. It is also found that TEO achieves the best emission gas reduction with 0.2137 ton/h compared to other techniques. The optimized value of emission gas was

achieved at a competitive time. The convergence behaviors for TEG minimization using the proposed method and other methods are illustrated in Fig. 6.

• **Test Case 3: Total Active Power Losses Minimization**

The third fitness function investigated was to reduce the total APL. The optimal results found using the proposed TEO and other techniques are shown in Table IX. It should be mentioned that the best optimal solution has been obtained by the presented method (TEO) with a value of 3.4976 MW. Fig. 7 shows the convergence characteristics for total real power loss minimization using PSO, GA, SSA, FDB-AEO, FDB-AOA, and TEO methods.

• **Test Case 4: Voltage Deviation Reduction**

In this test case, the voltage deviation was selected as the fitness function. Table X shows the optimized decision variables found using the proposed TEO and other techniques. It can be noticed that the TEO method achieves the best optimum with a value of 0.67514 p.u. Noting that the values obtained by all methods are almost the same. Fig. 8 illustrates the convergence characteristics for TVD minimization using the proposed TEO and other techniques.

Table XI displays a summary of the comparison between the optimized-results achieved by the presented method (TEO) and the other investigated techniques for single-fitness function on IEEE 30-bus test system.

• **Discussion of the Results**

The simulation results clearly demonstrated the superiority of the proposed method (TEO) when compared to other powerful population metaheuristic algorithms. It can be observed that the proposed TEO can solve with accuracy various single-objective functions-based OPF problems. It also provides a lower value for the majority of test cases studied. On the other hand, the proposed

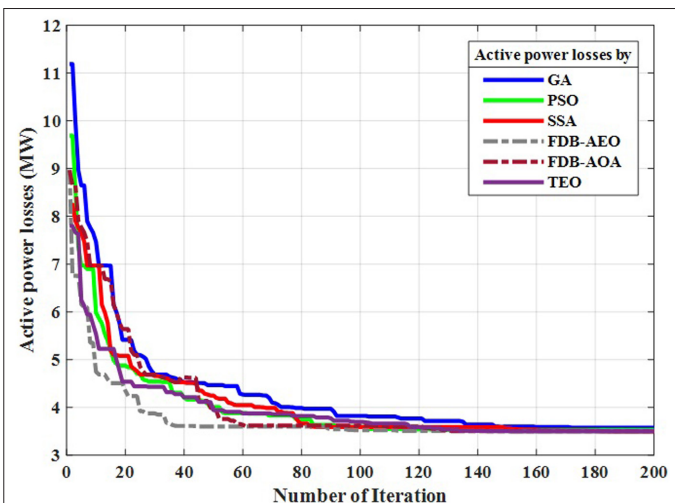


Fig. 7. Convergence behaviors for total power loss minimization: test case 3.

TABLE X THE OPTIMIZED RESULTS OF THE PROPOSED TECHNIQUE (TEO) AND OTHER METHODS: TEST CASE 4

PGi (MW)	GA	PSO	SSA	FDB-AEO	FDB-AOA	TEO
PG1	194.0816	159.4153	169.6567	189.3845	168.2957	173.1889
PG2	25.2490	80.0000	74.3248	50.8421	72.8975	71.4215
PG5	35.0760	15.0000	15.2995	20.5075	15.7564	15.0800
PG8	15.5173	13.5643	10.4383	10.3819	13.3754	11.4022
PG11	10.8967	11.4546	10.0772	10.6836	10.5875	10.7081
PG13	12.3078	13.5325	13.8788	12.2959	12.5457	12.0000
Total fuel cost (\$/h)	825.5293	823.6236	817.9730	804.4774	815.7353	815.1328
Emission gas (ton/h)	0.4204	0.3290	0.3598	0.4069	0.3553	0.3673
Active power losses (MW)	9.7284	9.5667	10.2753	10.6954	10.0582	10.4008
ΔV (p.u.)	0.6806	0.6789	0.6754	0.6754	0.6765	0.6751
CPU time (s)	22.6669	18.5927	17.4028	17.654262	18.4908	17.0174

GA, genetic algorithm; FDB-AEO, fitness-distance balance-based artificial ecosystem optimization; FDB-AOA, fitness-distance balance-based Archimedes optimization algorithm; PSO, particle swarm optimization; SSA, salp swarm algorithm; TEO, thermal exchange optimization. Bold values in Table X indicate the best value obtained.

TEO achieves the best solutions at a competitive computational time compared to other algorithms. It should be mentioned that in the majority of test cases, the optimum solutions have been achieved by using the TEO, among other competitive methods. The TEO algorithm has the best performance in terms of optimal solution, convergence, and minimum execution time. Therefore, it may be considered as a strong and competitive tool to solve various OPF problems.

• Robustness of the Proposed Method (TEO)

A statistical analysis is performed to measure the robustness and prove the efficiency of each method, in particular the TEO in solving various problems related to optimal power management. Four indices are calculated: the minimum, the maximum, the median, and the standard deviation (SD) for 50 independent runs. As well

depicted in Table XII, the proposed TEO achieved the best solution at a lower SD (0.03361) compared to other competitive methods. Fig. 9 shows the evolution of optimized TFC versus trials related to the proposed TEO and to other techniques. Fig. 10 illustrates a comparison between the optimized TFC versus trials for GA, TEO, SSA, PSO, and the two hybride optimization algorithms, namely FDB-AEO and FDB-AOA. It is confirmed that the reported technique (TEO) allows achieving the best solution at a reduced SD compared to other competitive methods. This clearly proves the accuracy and stability of this algorithm in solving various types of single-objective functions.

TABLE XI COMPARISON OF SIMULATION RESULTS BETWEEN TEO, SSA, GA, AND PSO FOR TEST CASES 1 TO 4

Methods	Total Fuel Cost (\$/h)	Emission Gas (ton/h)	Active Power Losses (MW)	Voltage Deviation (p.u.)
Initial	875.1688	0.8983	17.528	0.6380
Test case	Test case 1	Test case 2	Test case 3	Test case 4
GA	802.8716	0.2137	3.5761	0.6801
PSO	802.4219	0.2176	3.5259	0.6789
SSA	802.3603	0.2176	3.4979	0.6754
FDB-AEO	802.3604	0.2176	3.5065	0.6754
FDB-AOA	802.3883	0.2176	3.5045	0.6765
TEO	802.3607	0.2193	3.4976	0.6751

GA, genetic algorithm; FDB-AEO, fitness-distance balance-based artificial ecosystem optimization; FDB-AOA, fitness-distance balance-based Archimedes optimization algorithm; PSO, particle swarm optimization; SSA, salp swarm algorithm; TEO, thermal exchange optimization.

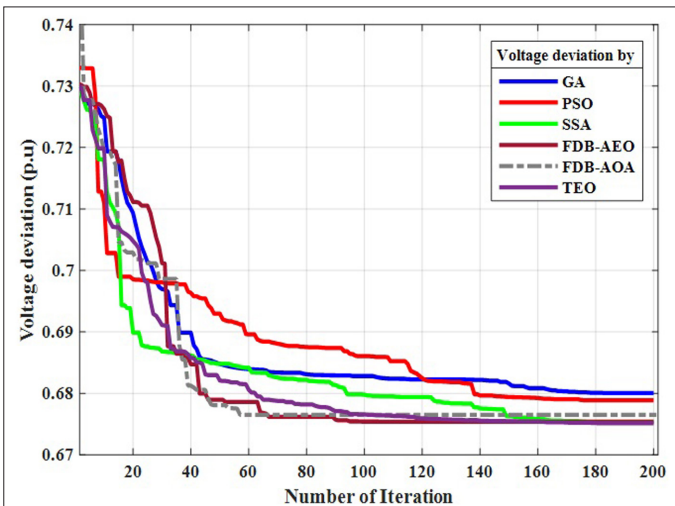


Fig. 8. Convergence behaviors for TVD: test case 4.

TABLE XII STATISTICAL ANALYSIS OF TEO AND OTHER METAHEURISTIC ALGORITHMS

	GA	PSO	SSA	FDB-AEO	FDB-AOA	TEO
Mean	803.5740	802.9784	802.4023	802.5861	802.8336	802.4007
Best	802.8716	802.4219	802.3603	802.3604	802.3883	802.3607
Median	803.5873	802.9017	802.3956	802.4575	802.7317	802.3937
Max	804.5768	803.8347	802.5243	803.5488	803.8324	802.5286
SD	0.385200	0.382200	0.035402	0.2905	0.3745	0.03361

GA, genetic algorithm; FDB-AEO, fitness-distance balance-based artificial ecosystem optimization; FDB-AOA, fitness-distance balance- based Archimedes optimization algorithm; PSO, particle swarm optimization; SSA, salp swarm algorithm; TEO, thermal exchange optimization.

• Discussion of Results Using Statistical Analysis: Test Cases 1 to 4

In this section, for all test cases (cases 1-4), each candidate algorithm has been executed 10 times. For that, the boxplot graph is used to evaluate the robustness of the proposed algorithm, namely TEO compared to other algorithms in terms of dispersion of the solutions. Four statistical indices are calculated: the minimum, the maximum, the median, and the SD. Table XIII shows the statistical results for 10 independent runs for all methods. Fig. 11 illustrates the box plot of the

fitness values for the TEO and other algorithms such as: GA, PSO,SSA, FBD-AEO, and FBD-AOA. It can be concluded that the proposed TEO is statistically superior compared to other techniques and has exhibited a stable search performance in relatively all test cases for single- and multi-objective functions. It is confirmed that the reported technique (TEO) allows achieving the best solution at a reduced SD compared to other methods. This clearly proves the accuracy and stability of this algorithm in solving such single-objective functions. According to these preliminary results, it can be concluded that the proposed TEO algorithm can be successfully used to solve various OPF problems.

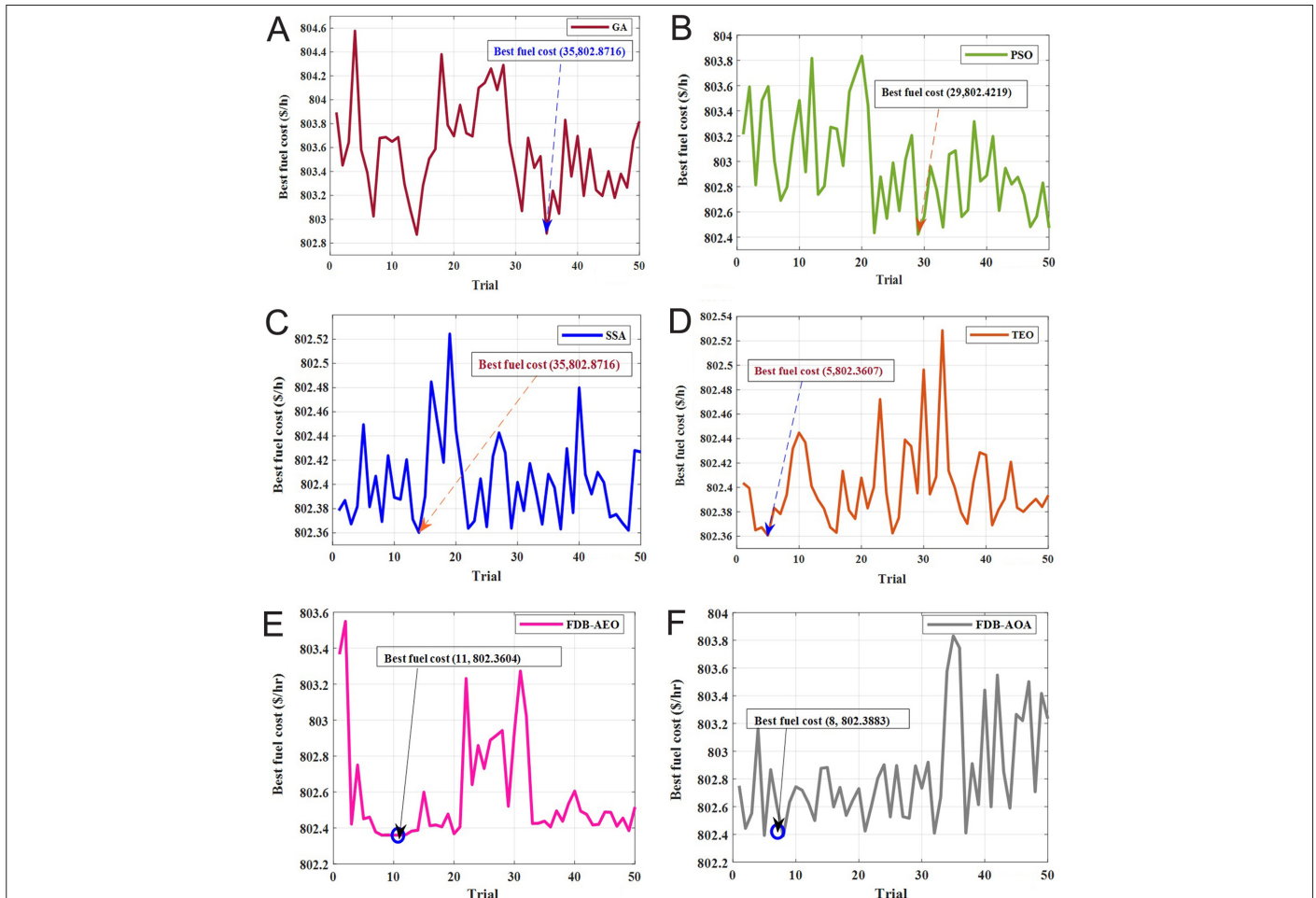


Fig. 9. Evolution of optimized TFC versus trials: (a) GA, (b) PSO, (c) SSA, (d) TEO, (e) FDB-AEO, (f) FDB-AOA.

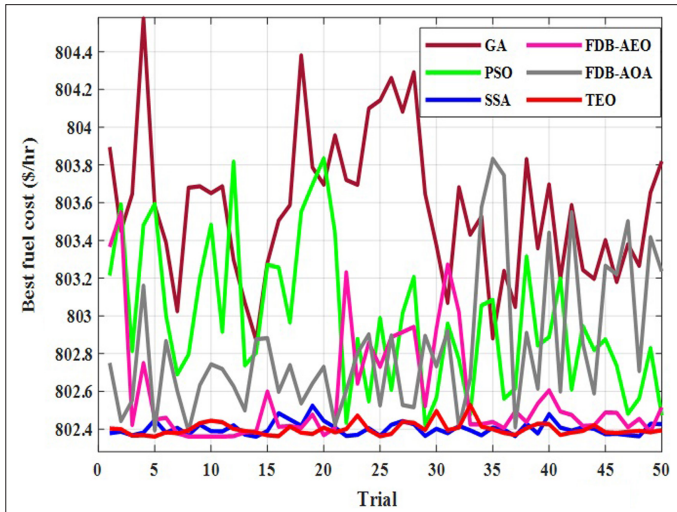


Fig. 10. Comparison between the optimized TFC versus trials for GA, TEO, SSA, PSO, FDB-AEO, and FDB-AOA.

2) Multi-Objective Optimal Power Flow Problem

As indicated earlier, the MOOPF has been used to improve the performance of practical power systems in terms of energy quality and operation’s security. A recent version of MOTE0 has been applied to solve various combined conflict bi-objective functions. The performance of the proposed MOTE0 has been verified and examined on the standard IEEE 30-bus test system. The population size is set to 20, and the iteration numbers are 200. The results will be presented, analyzed, and discussed in the following subsections.

• **Results and Discussions of Bi-Objective Function**

The efficiency of the proposed method (MOTE0) has been validated to optimize two objective functions simultaneously. To evaluate its ability and particularity, a comparative study has been carried out, and the results of the two-dimensional Pareto fronts of all three test cases provided by the MOTE0 are compared with other algorithms such as the MOGA, MOPSO, MSSA, DSC-MOAGDE, and IMOMRFO.

• **Test Case 5: Minimize TFC and TEG Simultaneously**

TABLE XIII STATISTICAL ANALYSIS FOR ALL SINGLE-OBJECTIVE CASES (1 TO 4) OF TEO AND OTHER METAHEURISTIC ALGORITHMS

Case		GA	PSO	SSA	FDB-AEO	FDB-AOA	TEO
1	Mean	803.5104	803.1650	802.4258	802.5184	802.8073	802.4074
	Best	802.8716	802.4219	802.3603	802.3604	802.3883	802.3607
	Median	803.5851	803.1084	802.4325	802.3782	802.6757	802.3966
	Max	804.5768	803.8347	802.5243	803.5488	803.8324	802.5286
	SD	0.5152	0.4502	0.0550	0.3884	0.4171	0.0511
2	Mean	0.2201	0.2177	0.2176	0.2178	0.2179	0.2165
	Best	0.2193	0.2175	0.2176	0.2176	0.2176	0.2137
	Median	0.2199	0.2177	0.2176	0.2177	0.2176	0.2172
	Max	0.2209	0.2179	0.2178	0.2188	0.2192	0.2183
	SD	5.3991e-04	1.0529e-04	8.3593e-05	3.5997e-04	6.2058e-04	0.0018
3	Mean	3.5882	3.5495	3.5133	3.5291	3.5159	3.5036
	Best	3.5761	3.5259	3.4979	3.5053	3.5045	3.4976
	Median	3.5818	3.5370	3.5115	3.5185	3.5175	3.5009
	Max	3.6308	3.6507	3.5464	3.6423	3.5321	3.5183
	SD	0.0171	0.0375	0.0160	0.0406	0.0085	0.0074
4	Mean	0.6817	0.6798	0.6773	0.6762	0.6774	0.6756
	Best	0.6806	0.6789	0.6754	0.6754	0.6765	0.6751
	Median	0.6816	0.6797	0.6777	0.6763	0.6771	0.6754
	Max	0.6856	0.6813	0.6797	0.6772	0.6799	0.6763
	SD	0.0014	7.7405e-04	0.0014	6.6073e-04	0.0012	4.7044e-04

GA, genetic algorithm; FDB-AEO, fitness-distance balance-based artificial ecosystem optimization; FDB-AOA, fitness-distance balance-based Archimedes optimization algorithm; PSO, particle swarm optimization; SSA, salp swarm algorithm; TEO, thermal exchange optimization.

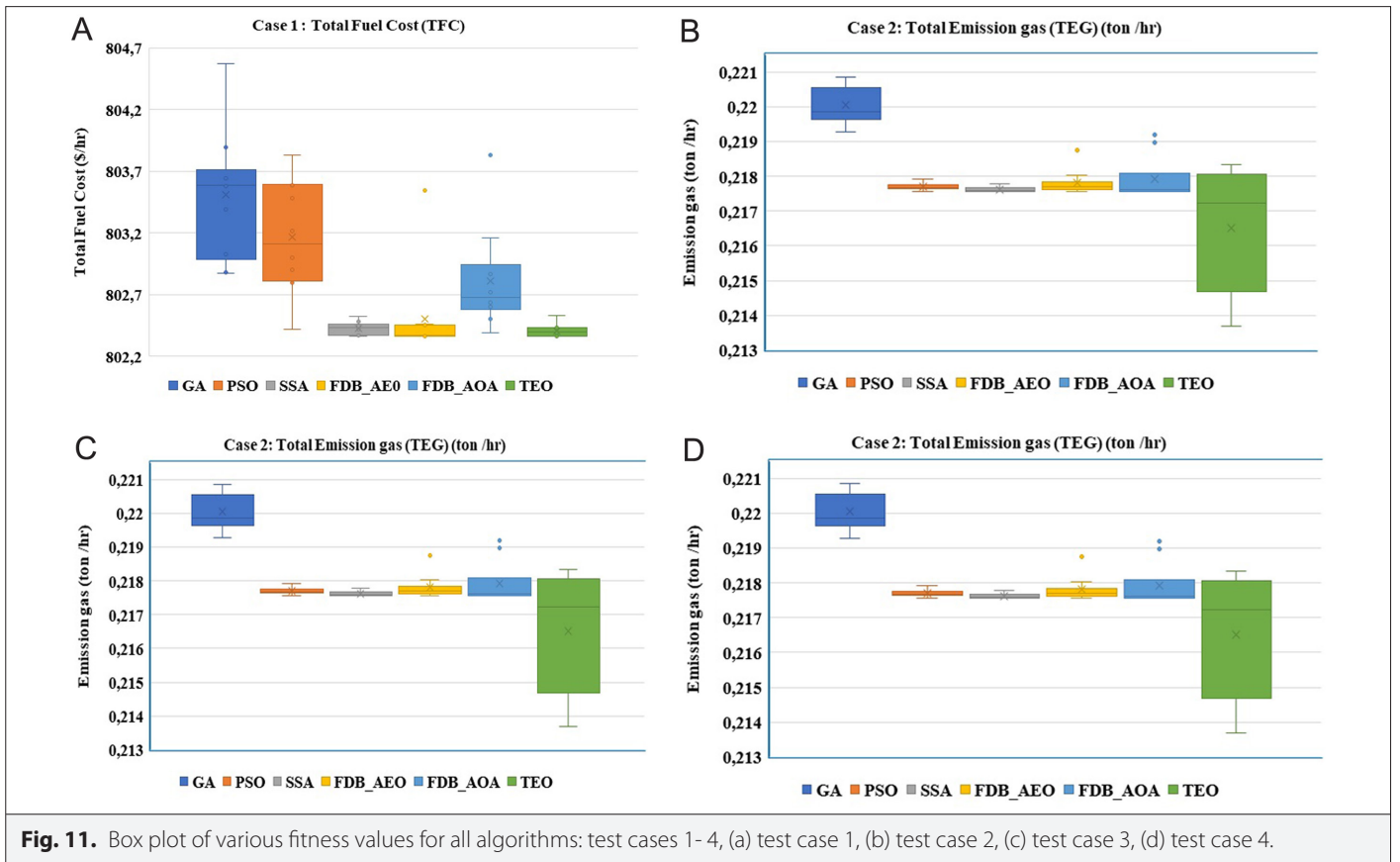


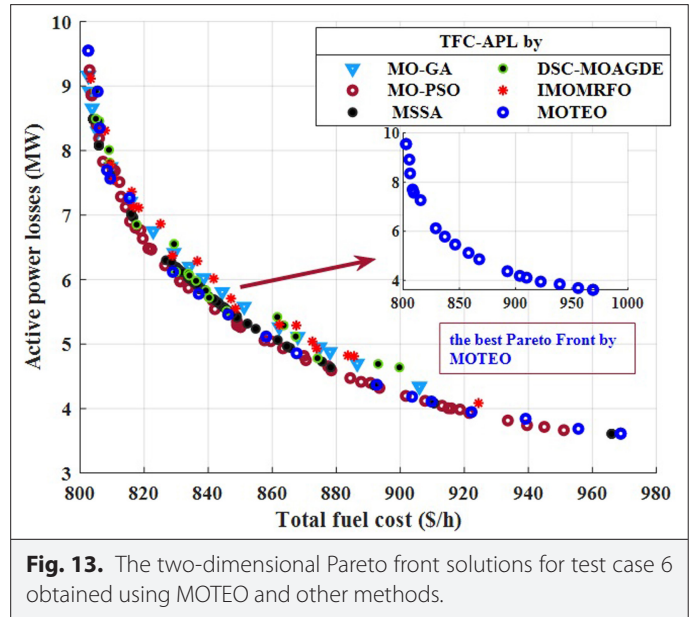
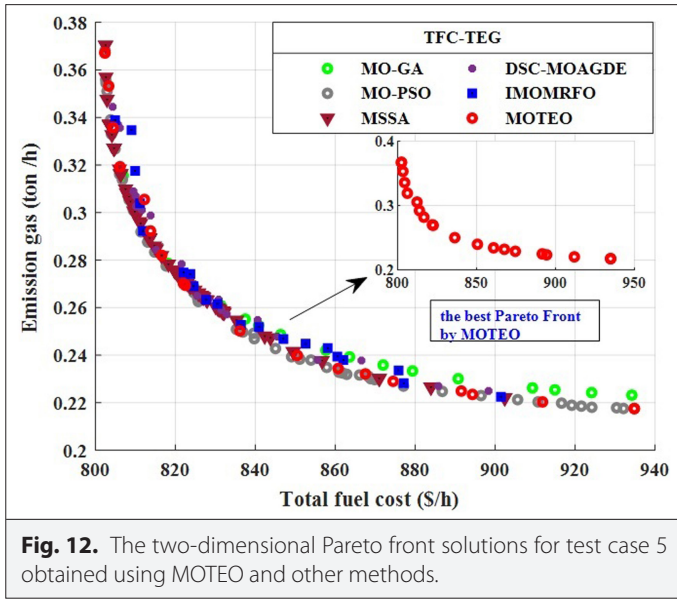
Fig. 11. Box plot of various fitness values for all algorithms: test cases 1- 4, (a) test case 1, (b) test case 2, (c) test case 3, (d) test case 4.

TABLE XIV COMPARISON OF OPTIMIZED BI-OBJECTIVE SOLUTION-BASED TFC AND TEG: TEST CASE 5

PGi (MW)	MOGA	MOPSO	MSSA	DSC-MOAGDE	IMOMRFO	MOTEO
PG1	11h8.9466	119.5862	129.7038	124.3816	123.6978	129.0920
PG2	60.1173	65.9017	56.7952	51.6604	73.7514	61.2001
PG5	33.5915	28.2659	30.7532	34.9932	19.9763	26.4864
PG8	27.1607	33.1777	30.2075	33.1353	27.5029	31.3122
PG11	23.4719	25.5318	21.9756	18.3483	22.2963	25.5441
PG13	26.1024	17.1631	20.4509	26.9306	23.0856	16.4142
Total fuel cost(\$/h)	837.4416	831.0422	823.7553	834.6016	831.5045	822.4796
Total cost (\$/h)	977.9700	973.0574	971.84984	978.6653	979.5550	970.8219
Emission gas(ton/h)	0.2552	0.2579	0.26894	0.26162	0.26886	0.26939
Active power losses (MW)	5.9904	6.2264	6.4862	6.0494	6.9104	6.6490
ΔV (p.u.)	0.7112	0.7105	0.7075	0.6691	0.6687	0.7091
CPU time (s)	29.9906	32.4147	19.4735	32.7852	34.3546	30.7970

IMOMRFO, improved multi-objective manta-ray foraging optimization; MOGA, multi-objective genetic algorithm; MOPSO, multi-objective particle swarm optimization; MSSA, multi-objective salp swarm algorithm; MOAGDE, multi-objective adaptive guided differential evolution; MOTEO, multi-objective thermal exchange optimization.

Bold values in Table X indicate the best value obtained.



The aim of this test case is to optimize two fitness functions, the TFC (\$/h) and the TEG (ton/h), simultaneously. The simulation results are provided in Table XIV. The Pareto fronts generated using the proposed MOTEO and other techniques are presented in Fig. 12. Table XIV depicts the optimized results obtained by MOTEO compared with other algorithms. It is found that MOTEO has the highest economic total cost (970.82189 \$/h) compared to other techniques.

• **Test Case 6: Minimizing the TFC and APL Simultaneously**

This case focuses on the optimization of the TFC (\$/h) and the total APL (MW). The optimal solutions for the two-dimensional Pareto fronts created by the proposed algorithm and other algorithms are shown in Fig. 13. Table XV gives the optimized tradeoff values of

control variables achieved by the proposed MOTEO and other multi-objective algorithms.

• **Test Case 7: Minimizing the APL and the VD Simultaneously**

This test case is dedicated to analyzing the conflict existing between the APL (MW) and the VD (p.u.). The statistical results of the simulation for this test case are depicted in Table XVI. Fig. 14 illustrates the two-Dimensional Pareto fronts generated by the presented algorithm (TEO) compared with other algorithms.

Table XVI represents a comparative study between MOTEO and other metaheuristic algorithms.

TABLE XV COMPARISON OF OPTIMIZED BI-OBJECTIVE SOLUTION BASED TFC AND APL: TEST CASE 6

PGi (MW)	MOGA	MOPSO	MSSA	DSC-MOAGDE	IMOMRFO	MOTEO
PG1	132.7925	122.3352	117.4630	133.9546	122.3850	127.1674
PG2	54.0488	58.4186	58.7366	49.4046	62.8179	47.6816
PG5	32.7928	38.1387	34.9059	33.5581	28.4283	30.8446
PG8	29.4633	34.4243	31.1443	22.4309	30.1119	35.0000
PG11	17.3037	18.6077	21.8392	23.8560	22.8256	26.5488
PG13	23.5788	17.4201	25.1411	26.7483	23.2041	22.2764
Total fuel cost (\$/h)	824.4156	837.8367	838.8245	829.317	828.8290	828.9341
Total emission gas (ton/h)	0.2739	0.2595	0.2531	0.2740	0.2608	0.2631
Active power losses (MW)	6.5799	5.9444	5.8302	6.5526	6.3728	6.1188
ΔV (p.u.)	0.7030	0.7038	0.7104	0.6720	0.6715	0.6770
CPU time (s)	31.7540	31.7991	18.6996	34.8751	32.1245	31.497

IMOMRFO, improved multi-objective manta-ray foraging optimization; MOGA, multi-objective genetic algorithm; MOPSO, multi-objective particle swarm optimization; MSSA, multi-objective salp swarm algorithm; MOTEO, multi-objective thermal exchange optimization; MOAGDE, multi-objective adaptive guided differential evolution.

TABLE XVI COMPARISON OF OPTIMIZED BI-OBJECTIVE SOLUTION-BASED APL AND VD: TEST CASE 7

PGi (MW)	MOGA	MOPSO	MOSSA	DSC-MOAGDE	IMOMRFO	MOTEO
PG1	76.4181	74.0321	99.6784	108.5225	100.3876	57.1299
PG2	75.9677	78.0799	73.6429	51.2789	63.2410	80.0000
PG5	49.9982	49.1559	42.8278	49.6713	45.0850	50.0000
PG8	34.4495	35.0000	26.6675	25.4817	26.5437	33.7980
PG11	25.5862	11.5237	16.0669	22.7374	26.3753	26.2274
PG13	25.1417	39.9856	29.8292	30.5887	26.5988	40.0000
Total fuel cost (\$/h)	921.0733	933.8563	876.8233	885.3373	877.4701	959.9527
Total emission gas (ton/h)	0.2226	0.2331	0.2418	0.2421	0.2349	0.2235
Active power losses (MW)	4.1614	4.3772	5.3127	4.9856	4.937	3.7553
ΔV (p.u.)	0.7173	0.7022	0.7041	0.7129	0.7158	0.7198
CPU time (s)	30.8146	32.8041	22.9968	32.8756	31.8754	30.7970

IMOMRFO, improved multi-objective manta-ray foraging optimization; MOGA, multi-objective genetic algorithm; MOPSO, multi-objective particle swarm optimization; MOSSA, multi-objective salp swarm algorithm; MOTEO, multi-objective thermal exchange optimization. Bold values in Table X indicate the best value obtained.

Table XVII shows a comparison study between optimized results achieved by the reported method (MOTEO) and other techniques.

• Discussion of Obtained Results

According to the simulation results focused on solving the MOOPF problems, three test cases have been studied to solve two conflicting objective functions simultaneously.

In the test case 5, the bi-objective function focused on solving the tradeoff between the TFC and TEG. Based on the results depicted in Table XIV, it can be noticed that the MOTEO achieved the better optimum compromise solution with a TFC value of 822.4796 \$/h and a TEG value of 0.26939 ton/h, which yields a reduced total fuel cost (970.8218974 \$/h) compared to those obtained by other algorithms. Fig. 12 depicts the tradeoff curve between the total fuel cost and emissions gas obtained by the MOTEO and other methods. It can be seen that MOTEO has the best Pareto optimal front with a highly uniform distribution.

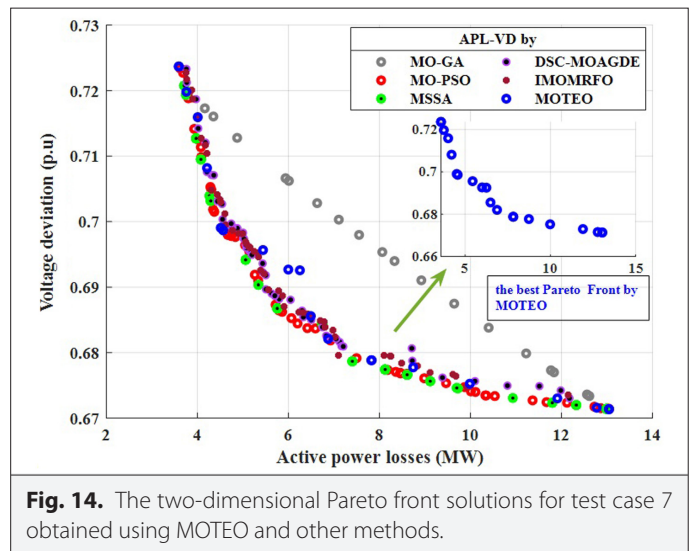


Fig. 14. The two-dimensional Pareto front solutions for test case 7 obtained using MOTEO and other methods.

TABLE XVII A COMPARATIVE STUDY BETWEEN MOTEO WITH OTHER METAHEURISTIC ALGORITHMS

Test Cases		MOGA	MOPSO	MOSSA	DSC-MOAGDE	IMOMRFO	MOTEO
5	TFC (\$/h)	837.4416	831.0422	823.7553	834.6016	831.5045	822.4796
	TEG (ton/h)	0.2552	0.25790	0.26894	0.26162	0.26886	0.26939
	Total cost (\$/h)	977.9700	973.0574	971.8498	978.6653	979.5550	970.8219
6	TFC (\$/h)	824.4156	837.8367	838.8245	829.317	828.8290	828.9341
	APL (MW)	6.5799	5.9444	5.8302	6.5526	6.3728	6.1188
7	APL (MW)	4.1614	4.3772	5.3127	4.9856	4.937	3.7553
	VD (p.u.)	0.7173	0.7022	0.7041	0.7129	0.7158	0.7198

IMOMRFO, improved multi-objective manta-ray foraging optimization; MOGA, multi-objective genetic algorithm; MOPSO, multi-objective particle swarm optimization; MOSSA, multi-objective salp swarm algorithm; MOTEO, multi-objective thermal exchange optimization.

TABLE XVIII COMPARATIVE BEST COMPROMISE SOLUTION-BASED THREE-DIMENSIONAL PARETO FRONTS GENERATED BY THE MOTEO

PGi (MW)	Best Total Fuel Cost	Best Emission Gas	Best Active Power Losses	Best Compromise Solution
PG1	176.4878	70.1690	51.9111	113.8162
PG2	48.8374	71.4234	79.9957	69.9688
PG5	21.4310	49.1068	49.9983	35.1111
PG8	21.9482	34.6021	34.9973	33.5876
PG11	12.1969	28.2083	29.9984	24.7972
PG13	12.0000	33.8037	39.9968	12.0000
Total fuel cost (\$/h)	802.3607	929.7806	968.5297	844.3766
Emission gas (ton/h)	0.3665	0.21929	0.2216	0.25262
Active power losses (MW)	9.5012	3.9134	3.4976	5.8808
ΔV (p.u.)	0.6829	0.7219	0.7237	0.6690
CPU time (s)	16.9921	17.2861	17.2302	37.1027

Bold values in Table X indicate the best value obtained.

In test case 6, the bi-objective function focused on solving the trade-off between the total fuel cost and the total APL. As can be seen from Table XV, the best optimum compromise solution for this test case obtained using the proposed MOTEO is: 828.9341 \$/h for TFC and 6.1188 MW for APL, respectively. Fig. 13 shows the optimal Pareto front generated by MOTEO and other techniques. These solutions cover a wider range of the entire Pareto front with uniform distribution solutions.

In test case 7, investigate the application of the proposed MOTEO for solving the bi-objective functions based on total power losses and voltage deviation. Table XVI presents the best optimum compromise solution achieved by using the proposed algorithm compared to other techniques. The best compromise solutions obtained by MOTEO are 3.7553 MW for APL and 0.71982 p.u. for VD. Fig. 14 shows the distribution of the two-dimensional Pareto front solutions of the APL and the VD. It can be seen clearly that MOTEO has a higher uniform distribution Pareto optimal front compared to other algorithms. The results provided by the proposed method (MOTEO) clearly demonstrate the superiority of this algorithm over other algorithms. The MOTEO achieved the best compromise solution for all test case-based bi-objective functions compared to other algorithms, but it is slightly better than the MSSA. Also, it can be shown clearly that MOTEO has provided the highest Pareto front with uniform distribution solutions and covers a wider range of fitness functions studied.

• **Test case 8: Minimization of three objective functions: Total fuel cost, Total emission gas, and active power losses**

This test case is focused to validate the particularity of the proposed technique by applying it to simultaneously optimizing three objective functions: the TFC, the total power losses, and the TEG. Table XVIII summarizes the optimized results for the best compromise solutions. The three-dimensional Pareto fronts achieved by the MOTEO are illustrated in Fig. 15.

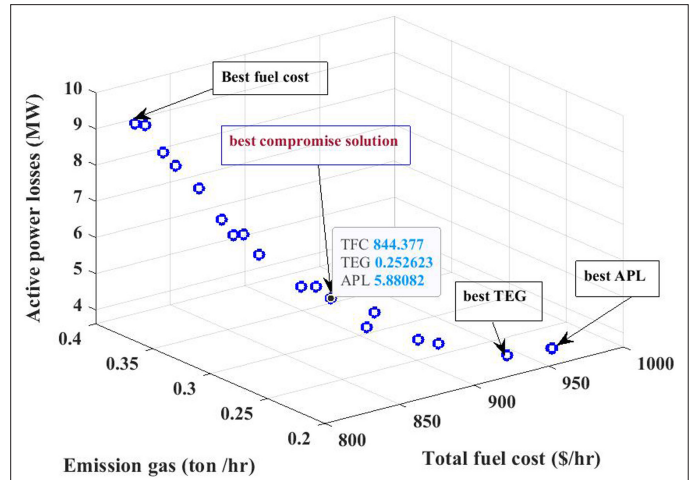


Fig. 15. The three-dimensional Pareto fronts-based MOTEO: test case 8.

V. CONCLUSION

In this research paper, a novel meta-heuristic approach, namely the TEO algorithm, inspired by physical phenomena, has been successfully adapted and applied to improve the solution of multi-objective OPF problems. The reported algorithm has been implemented and validated on the standard IEEE 30-bus test system to optimize various fitness functions such as the TFC, TEG, APL, and DV. The simulation results of single-objective-based OPF confirmed that the TEO could efficiently achieve competitive solutions compared to other techniques in terms of solution accuracy and execution time. The TEO can get the best solutions and provide considerably better values for all objective functions. Also, the execution time required by TEO for resolving each objective function is slightly faster than other competitive algorithms. Moreover, the MOTEO has been investigated for solving combined objective functions-based OPF, and it is also examined through optimizing tri-objective functions. The obtained results clearly indicate that the presented method is able to find a near-global solution by optimizing the control variables related to the standard IEEE 30-bus test system. The Pareto curve provided by solving combined objective functions allows the decision-maker to make a better-informed decision regarding the compromise between the conflicting objectives. It is found from all optimization results that the TEO has high performance to solve several OPF problems, including both single- and multi-objective OPF problems. Due to the competitive aspect of the proposed TEO, in the near future, this technique will be adapted and applied to solve the large-scale OPF of the Algerian electric test system, considering the integration of various types of renewable energy in coordination with the FACTS devices.

Peer-review: Externally peer-reviewed.

Author Contributions: Concept – Z.D., B.M.; Design – Z.D., B.M.; Supervision– Z.D., B.M.; Resources – B.M., K.S.; Materials – B.M., K.S.; Data Collection and/or Processing – Z.D., B.M.; Analysis and/or Interpretation – Z.D., B.M.; Literature Search – Z.D., B.M.; Writing – Z.D., B.M.; Critical Review – Z.D., B.M.

Declaration of Interests: The authors have no conflict of interest to declare.

Funding: The authors declared that this study has received no financial support.

REFERENCES

1. S. C. Kim, and S. R. Salkut, "Optimal power flow based congestion management using enhanced genetic algorithms," *Int. J. Electr. Comput. Eng.*, vol. 9, no. 2, pp. 2088–8708, 2019. [\[CrossRef\]](#)
2. H. Bakir, U. Guvenc, S. Duman, and H. T. Kahraman, "Optimal power flow for hybrid AC/DC electrical networks configured with VSC-MTDC transmission lines and renewable energy sources," *IEEE Syst. J.*, vol. 17, no. 3, pp. 3938–3949, 2023. [\[CrossRef\]](#)
3. M. H. Ali, A. M. El-Rifaie, A. A. F. Youssef, V. N. Tulsy, and M. A. Tolba, "Techno-economic strategy for the load dispatch and power flow in power grids using peafowl optimization algorithm," *Energies*, vol. 16, no. 2, p. 846, 2023. [\[CrossRef\]](#)
4. S. Duman, H. T. Kahraman, and M. Kati, "Economical operation of modern power grids incorporating uncertainties of renewable energy sources and load demand using the adaptive fitness-distance balance-based stochastic fractal search algorithm," *Eng. Appl. Artif. Intell.*, vol. 117, p. 105501, 2023. [\[CrossRef\]](#)
5. S. Liu, C. Wu, and H. Zhu, "Topology-aware graph neural networks for learning feasible and adaptive AC-OPF solutions," *IEEE Trans. Power Syst.*, vol. 38, no. 6, 5660–5670, 2022. [\[CrossRef\]](#)
6. A. M. Shaheen, R. A. El-Sehiemy, H. M. Hasanien, and A. R. Ginidi, "An improved heap optimization algorithm for efficient energy management based optimal power flow model," *Energy*, vol. 250, p. 123795, 2022. [\[CrossRef\]](#)
7. S. B. Pandya, and H. R. Jariwala, "A different perception of hybrid renewable energy sources integrated multi-objective optimal power flow considering performance parameters and penetration," *Smart Sci.*, vol. 9, no. 3, pp. 186–215, 2021. [\[CrossRef\]](#)
8. H. Bakir, U. Guvenc, and H. T. Kahraman, "Optimal operation and planning of hybrid AC/DC power systems using multi-objective grasshopper optimization algorithm," *Neural Comput. Appl.*, vol. 34, no. 24, pp. 22531–22563, 2022. [\[CrossRef\]](#)
9. S. Li, W. Gong, L. Wang, and Q. Gu, "Multi-objective optimal power flow with stochastic wind and solar power," *Appl. Soft Comput.*, vol. 114, p. 108045, 2022. [\[CrossRef\]](#)
10. T. H. B. Huy, D. Kim, and D. N. Vo, "Multiobjective optimal power flow using multiobjective search group algorithm," *IEEE Access*, vol. 10, pp. 77837–77856, 2022. [\[CrossRef\]](#)
11. B. Mallala, V. P. Papan, R. Sangu, K. Palle, and V. K. R. Chinthalachervu, "Multi-objective optimal power flow solution using a non-dominated sorting hybrid fruit fly-based artificial bee colony," *Energies*, vol. 15, no. 11, p. 4063, 2022. [\[CrossRef\]](#)
12. F. Daqaq, M. Ouassaid, and R. Ellaia, "A new meta-heuristic programming for multi-objective optimal power flow," *Electr. Eng.*, vol. 103, no. 2, pp. 1217–1237, 2021. [\[CrossRef\]](#)
13. H. K. Ahmad, "Ac power flow analysis using fast decoupled Newton-Raphson algorithm compared with Gaussian-Seidel approach," *J. Optoelectron. Laser*, vol. 41, no. 3, 2022.
14. M. Riaz et al., "An optimal power flow solution of a system integrated with renewable sources using a hybrid optimizer," *Sustainability*, vol. 13, no. 23, p. 13382, 2021. [\[CrossRef\]](#)
15. N. Salehi, H. Martínez-García, G. Velasco-Quesada, and J. M. Guerrero, "A comprehensive review of control strategies and optimization methods for individual and community microgrids," *IEEE Access*, vol. 10, pp. 15935–15955, 2022. [\[CrossRef\]](#)
16. O. Akdag, "A improved Archimedes optimization algorithm for multi/single-objective optimal power flow," *Electr. Power Syst. Res.*, vol. 206, p. 107796, 2022. [\[CrossRef\]](#)
17. A. Si Tayeb, B. Larouci, D. Rezzak, Y. Houam, H. Bouzeboudja, and A. Bouchakour, "Application of a new hybridization to solve economic dispatch problem on an Algerian power system without or with connection to a renewable energy," *Diagnostyka*, vol. 22, no. 3, pp. 101–112, 2021. [\[CrossRef\]](#)
18. Z. Lan, Q. He, H. Jiao, and L. Yang, "An improved equilibrium optimizer for solving optimal power flow problem," *Sustainability*, vol. 14, no. 9, p. 4992, 2022. [\[CrossRef\]](#)
19. T. Jumani, M. Mustafa, M. Rasid, N. Mirjat, M. Baloch, and S. Salisu, "Optimal power flow controller for grid-connected microgrids using grasshopper optimization algorithm," *Electronics*, vol. 8, no. 1, p. 111, 2019. [\[CrossRef\]](#)
20. H. R. E. H. Bouchekara, A. E. Chaib, and M. A. Abido, "Optimal power flow using GA with a new multi-parent crossover considering: Prohibited zones, valve-point effect, multi-fuels and emission," *Electr. Eng.*, vol. 100, no. 1, pp. 151–165, 2018. [\[CrossRef\]](#)
21. E. Naderi, M. Pourakbari-Kasmaei, and H. Abdi, "An efficient particle swarm optimization algorithm to solve optimal power flow problem integrated with FACTS devices," *Appl. Soft Comput.*, vol. 80, pp. 243–262, 2019. [\[CrossRef\]](#)
22. K. Padma, and Y. Shiferaw, "A solution to optimal power flow problem using metaheuristic bat algorithm," *National Scientific Conference on Emerging Technology (ET)*, vol. 3, no. 3, pp. 87–91, 2019.
23. E. H. Houssein, M. H. Hassan, M. A. Mahdy, and S. Kamel, "Development and application of equilibrium optimizer for optimal power flow calculation of power system," *Appl. Intell. (Dordr)*, vol. 53, no. 6, pp. 7232–7253, 2023. [\[CrossRef\]](#)
24. Y. A. N. G. Bo, W. A. N. G. Junting, Y. U. Lei, C. A. O. Pulin, S. H. U. Hongchun, and Y. U. Tao, "Peafowl optimization algorithm based bi-level multi-objective optimal allocation of energy storage systems in distribution network," *J. Shanghai Jiaotong Univ.*, vol. 56, no. 10, p. 1294, 2022.
25. S. Duman, H. T. Kahraman, Y. Sonmez, U. Guvenc, M. Kati, and S. Aras, "A power flow meta-heuristic search algorithm for solving global optimization and real-world solar photovoltaic parameter estimation problems," *Eng. Appl. Artif. Intell.*, vol. 111, p. 104763, 2022. [\[CrossRef\]](#)
26. G. Eappen, and S. T. Shankar, "Hybrid PSO-GSA for energy efficient spectrum sensing in cognitive radio network" *Phys. Commun.*, vol. 40, p. 101091, 2020. [\[CrossRef\]](#)
27. S. S. Reddy, "Optimal power flow using hybrid differential evolution and harmony search algorithm," *Int. J. Mach. Learn. Cybern.*, vol. 10, no. 5, pp. 1077–1091, 2019. [\[CrossRef\]](#)
28. M. Gao, J. Yu, Z. Yang, and J. Zhao, "A physics-guided graph convolution neural network for optimal power flow," *IEEE Trans. Power Syst.*, vol. 0885–8950, p. 1–11, 2023. [\[CrossRef\]](#)
29. S. Birolgul, "Hybrid harris hawk optimization based on differential evolution (HHODE) algorithm for optimal power flow problem," *IEEE Access*, vol. 7, pp. 184468–184488, 2019. [\[CrossRef\]](#)
30. H. Bakir, S. Duman, U. Guvenc, and H. T. Kahraman, "A novel optimal power flow model for efficient operation of hybrid power networks," *Comput. Electr. Eng.*, vol. 110, p. 108885, 2023. [\[CrossRef\]](#)
31. Y. Sonmez, S. Duman, H. T. Kahraman, M. Kati, S. Aras, and U. Guvenc, "Fitness-distance balance based artificial ecosystem optimisation to solve transient stability constrained optimal power flow problem," *J. Exp. Theor. Artif. Intell.*, pp. 1–40, 2022. [\[CrossRef\]](#)
32. U. Guvenc, S. Duman, H. T. Kahraman, S. Aras, and M. Kati, "Fitness-Distance Balance based adaptive guided differential evolution algorithm for security-constrained optimal power flow problem incorporating renewable energy sources," *Appl. Soft Comput.*, vol. 108, p. 107421, 2021. [\[CrossRef\]](#)
33. J. Zhang, S. Wang, Q. Tang, Y. Zhou, and T. Zeng, "An improved NSGA-III integrating adaptive elimination strategy to solution of many-objective optimal power flow problems," *Energy*, vol. 172, pp. 945–957, 2019. [\[CrossRef\]](#)
34. F. R. Zaro, and M. A. Abido, "Multi-objective particle swarm optimization for optimal power flow in a deregulated environment of power systems," In 11th International Conference on Intelligent Systems Design and Applications, IEEE Publications, 2011, pp. 1122–1127. [\[CrossRef\]](#)
35. S. Duman, M. Akbel, and H. T. Kahraman, "Development of the multi-objective adaptive guided differential evolution and optimization of the MO-ACOPF for wind/PV/tidal energy sources," *Appl. Soft Comput.*, vol. 112, p. 107814, 2021. [\[CrossRef\]](#)
36. H. T. Kahraman, M. Akbel, and S. Duman, "Optimization of optimal power flow problem using multi-objective manta ray foraging optimizer," *Appl. Soft Comput.*, vol. 116, p. 108334, 2022. [\[CrossRef\]](#)
37. M. H. Hassan, S. Kamel, J. L. Domínguez-García, M. F. El-Naggar, and MSSA-DEED, "MSSA-DEED: A multi-objective salp swarm algorithm for solving dynamic economic emission dispatch problems," *Sustainability*, vol. 14, no. 15, p. 9785, 2022. [\[CrossRef\]](#)
38. N. A. Zolpakar, S. S. Lodhi, S. Pathak, and M. A. Sharma, In *Optimization of Manufacturing Processes*. Cham: Springer, 2020, pp. 185–199.
39. B. Yenipinar, A. Şahin, Y. Sönmez, C. Yılmaz, and H. T. Kahraman, "Design optimization of induction motor with FDB-based Archimedes optimization algorithm for high power fan and pump applications," In *Smart Applications with Advanced Machine Learning and Human-Centred Problem Design*. Cham: Springer International Publishing, 2023, pp. 409–428. [\[CrossRef\]](#)

40. M., Al-Bahrani, L., V. Dumbrava, and M. Eremia, "Optimal power flow with four objective functions using improved differential evolution algorithm: Case study IEEE 57-bus power system", 10th International Conference on ENERGY and ENVIRONMENT (CIEM). IEEE Publications, 2021, pp. 1–5.
41. G. Chen, J. Qian, Z. Zhang, and S. Li, "Application of modified pigeon-inspired optimization algorithm and constraint-objective sorting rule on multi-objective optimal power flow problem," *Appl. Soft Comput.*, vol. 92, p. 106321, 2020. [\[CrossRef\]](#)
42. S. P. Dash, K. R. Subhashini, and P. Chinta, "Development of a Boundary Assigned Animal Migration Optimization algorithm and its application to optimal power flow study," *Expert Syst. Appl.*, vol. 200, p. 116776, 2022. [\[CrossRef\]](#)
43. H. T. Kahraman, and S. Duman, "Multi-objective adaptive guided differential evolution for multi-objective optimal power flow incorporating wind-solar-small hydro-tidal energy sources," In *Differential Evolution: From Theory to Practice*. Singapore: Springer Nature Singapore, 2022, pp. 341–365. [\[CrossRef\]](#)
44. S. S. Reddy, "Multi-objective optimal power flow for a thermal-wind-solar power system," *J. Green Eng.*, vol. 7, no. 4, pp. 451–476, 2017.
45. S. Duman, H. T. Kahraman, U. Guvenc, and S. Aras, "Development of a Lévy flight and FDB-based coyote optimization algorithm for global optimization and real-world ACOPF problems," *Soft Comput.*, vol. 25, no. 8, pp. 6577–6617, 2021. [\[CrossRef\]](#)
46. R. K. Avvari, and D. M., "Multi-Objective Optimal Power Flow including Wind and Solar Generation Uncertainty Using New Hybrid Evolutionary Algorithm with Efficient Constraint Handling Method," *Int. Trans. Electr. Energy Syst.*, vol. 2022, 1–15, 2022. [\[CrossRef\]](#)
47. S. S. Reddy, and P. R. Bijwe, "An efficient optimal power flow using bisection method," *Electr. Eng.*, vol. 100, no. 4, pp. 2217–2229, 2018. [\[CrossRef\]](#)
48. N. Khodadadi, S. Talatahari, and A. Dadras Eslamlou, "MOTEO: A novel multi-objective thermal exchange optimization algorithm for engineering problems," *Soft Comput.*, vol. 26, no. 14, pp. 6659–6684, 2022. [\[CrossRef\]](#)
49. N. Khodadadi, S. Talatahari, and A. D. Eslamlou, *A Novel Multi-objective Thermal Exchange Optimization Algorithm for Optimal Design of Truss Structures*, 2021.



Djebblahi Zahia was born in Biskra, Algeria. She received her Master degree in Electrical Engineering from Biskra University, Algeria in 2020, she is working towards her doctorate thesis in power system field. Her research interests include power system optimization, FACTS technology, Solar Photovoltaic and Wind sources modeling and integration in practical power system. Zahia.djebblahi@univ-biskra.com



Mahdad Belkacem was born in Biskra, Algeria. He received his B.S degree in Electrical Engineering from Biskra University, Algeria in 1990, and the Magister and Ph.D degrees from Annaba University and Biskra University in 2000 and 2010, respectively. He is a professor at Biskra University. His research interests include power system optimization, FACTS technology and Renewable sources modeling and integration in practical power system, Optimization methods, power system stability and system protection coordination. belkacem.mahdad@univ-biskra.dz



Kamel Srairi was born in Batna, Algeria, in 1967. He received the B.Sc. degree in Electrical Engineering, in 1991, from the University of Batna, Algeria; the M.Sc. degree in Electrical and Computer Engineering, from the National Polytechnic Institute of Grenoble, France, in 1992; and the Ph.D. degree also in Electrical and Computer Engineering, from the University of Nantes, France, in 1996. After graduation, he joined the University of Biskra, Algeria, in 1998 where he is a Professor in the Electrical Engineering Department. His main research interests include analysis, design, and control of electric system. k.srairi@univ-biskra.dz